Comprehensively Defining the Determinants of Neutralization by Broadly Cross-Reactive Flavivirus Antibodies

Jackson Barr Stuart

A thesis

submitted in partial fulfillment of the

requirements for the degree of

Master of Science

University of Washington

2021

Committee:

Leslie Goo

Jesse Bloom

Andrew McGuire

Program Authorized to Offer Degree:

Pathobiology

University of Washington

Abstract

Comprehensively Defining the Determinants of Neutralization by Broadly Cross-Reactive Flavivirus Antibodies

Jackson Barr Stuart

Chair of the Supervisory Committee:

Leslie Goo

Department of Global Health

Zika virus (ZIKV) and dengue virus (DENV) are two highly related mosquito-borne members of the genus *Flavivirus* that cause significant human morbidity and mortality. There is no licensed vaccine available for ZIKV and the sole vaccine available for DENV is suboptimal both in terms of its efficacy and safety. There is much interest in the development of a single vaccine effective against ZIKV and DENV as both viruses co-circulate due to shared vectors and vertebrate hosts, and due to the risk of antibody-dependent enhancement of subsequent infection by either virus. Two classes of broadly neutralizing antibodies (bnAbs) capable of potently neutralizing both viruses have recently been isolated: EDE-class and MZ4-class bnAbs. Through traditional epitope mapping methods, EDE bnAbs were found to bind to a conserved quaternary epitope found on the

flavivirus envelope protein (E) while MZ4 bnAbs bind to a linker region found between domain I and domain III of E protein. However, these mapping methods are only capable of providing data on binding and structural footprints. In order to better understand the determinants of neutralization for these bnAbs, I utilized a high-throughput approach called deep mutational scanning (DMS) that is capable of providing amino acid-resolution data on the determinants of neutralization – data that will be useful for further investigation of these bnAbs as potential therapeutics and as the basis for a cross-protective vaccine. I demonstrate the successful rescue of a ZIKV E protein virus library, the identification of an inhibitory concentration of 99% for both bnAbs, and the initial attempts at performing a DMS selection assay.

Table of Contents

List of Figures

List of Tables

Acknowledgements

I could write a separate thesis on the people who have aided, guided, and advised me on this journey. I cannot thank each and every one of you enough for all the time and energy you provided me throughout this journey. I am in awe at the caliber of scientists, trainees, support staff, and everyone else who I have come across during these two years. I will name a few below, but this truly is a cursory list and I want to express my upmost gratitude for everyone I have had the pleasure of interacting with here in Seattle. A special thank you goes out to my dissertation advisor, Dr. Leslie Goo, for her steadfast support during these trying times. I could not have asked for a better mentor, and I am so excited to see where this fledgling research group ends up. I have complete confidence in their success. I also want to thank:

- My graduate committee: Leslie Goo, Jesse Bloom, and Andy McGuire. Your words of advice and encouragement were invaluable.
- My program, particularly Lee Ann Campbell and Ernie Lefler.
- My family and loving partner. I love you all dearly; I hope to make y'all proud.
- The Bloom Lab (Fred Hutch), particularly David Bacsik, Rachel Eguia, and Jesse Bloom for all of your scientific advice.
- Members of the Goo Lab: Lisa Levoir, Jay Lubow, Laura Belmont, Lucas Contreras, and Caroline Kikawa. Thank you for all of the laughs and good times. Keep on doing some amazing research!
- Robin Kaai, for doing such an excellent rotation and setting me up for success.

Thank you, all!

Chapter 1. Introduction

1.1 Global epidemiology of ZIKV and DENV

Zika virus (ZIKV) and dengue virus (DENV) are two highly related mosquito-borne viruses that cause significant global morbidity and mortality (Pierson 2020). DENV specifically is estimated to infect 105 million people each year, and greater than a quarter of the globe's population lives in a DENV-endemic region (Cattarino 2020). Due to shared ecological niches including common vectors such as the mosquito *Aedes aegypti*, these two flaviviruses often co-circulate in endemic regions **(Figure 1)** and can oftentimes present indistinguishable symptoms (Pierson 2020). For the most part, infection by either ZIKV or DENV results in either an asymptomatic infection or a self-limiting febrile illness. In a reduced number of people, disease can progress to more serious outcomes such as microcephaly in infants or Guillain-Barré Syndrome with a ZIKV infection (Rawal 2016), or, with a DENV infection, disease can progress to potentially fatal dengue hemorrhagic fever and dengue shock syndrome (Bäck 2013).

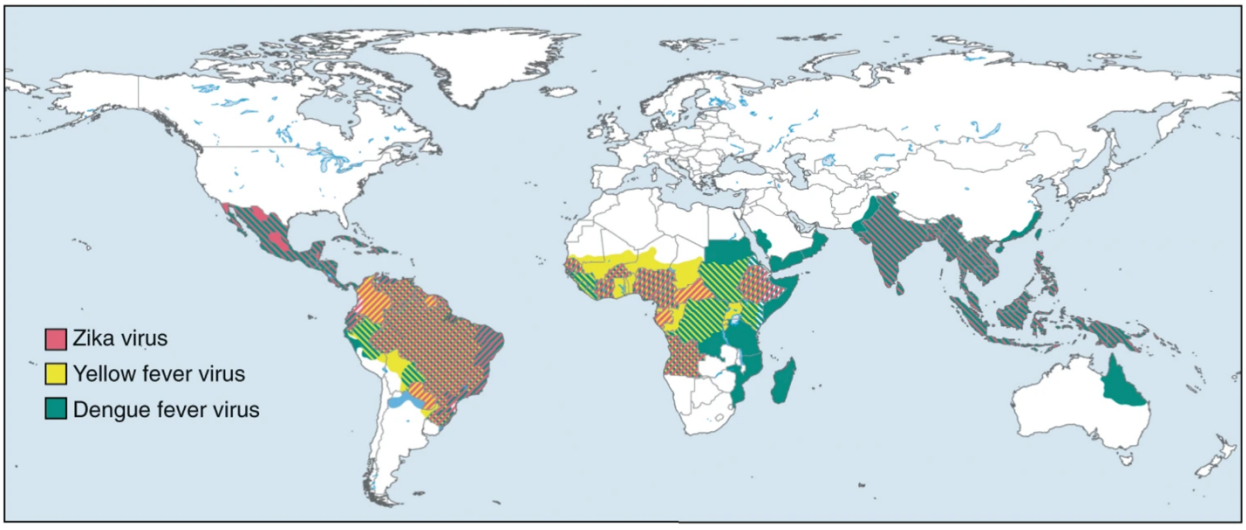

Figure 1. Global distribution of ZIKV and DENV. Figure sourced from Pierson 2020. ZIKV (red) and DENV (green) have shared ecological niches and significant geographic overlap. Yellow fever virus (yellow) – another flavivirus – is also shown.

Both ZIKV and DENV emerged from sylvatic cycles involving local mosquito vectors and non-human primates, though DENV has since fully adapted to its human host and the role of its sylvatic cycle in spurring endemic-epidemic cycles is uncertain (Guzman 2016). While DENV became distributed throughout the tropics in the 18th and 19th centuries, more recent globalization has resulted in rapid spread and the introduction of multiple serotypes – DENV1-4 – into overlapping regions (Guzman 2016). ZIKV was first isolated in 1947 in Uganda from a rhesus macaque and has caused sporadic outbreaks as recently as 2013 in French Polynesia (Musso 2018). In late 2013 or early 2014, ZIKV was introduced to South America and spurred a large epidemic in the Americas that peaked in 2016 and has resulted in the endemicity of ZIKV in the Central and South America (Zhang 2017). Since its peak, ZIKV cases have significantly diminished likely due to robust herd immunity within endemic regions (Metsky 2017). It remains an open question if ZIKV will enter into an epidemic-endemic cycle in Central and South America similar to DENV.

1.2 Flavivirus life cycle and structure

ZIKV and DENV are single-stranded, positive-sense, enveloped RNA viruses in the genus *Flavivirus* (family: *Flaviviridae*). These viruses, like all flaviviruses, are relatively small with an average diameter of 50 nm and a genome length of approximately 10.8 kilobases that encodes for 3 structural proteins – pre-membrane (prM), capsid (C), and

envelope (E) – as well as 7 nonstructural proteins – NS1, NS2A, NS2B, NS3, NS4A, NS4B, and NS5 (Sirohi 2017). These proteins are encoded in a single polyprotein that undergoes proteolytic cleavage by a combination of viral- and host-encoded proteins (Aktepe 2018). Of note, prM proteins associate with E proteins at a 1:1 ratio in order to prevent improper conformational changes during replication and assembly but are cleaved by host proteases into M proteins that remain associated with E dimers in the Golgi. On a fully "matured" flavivirus virion, 180 E proteins are dimerized and form an antiparallel raft-like structure that covers the surface of the virion.

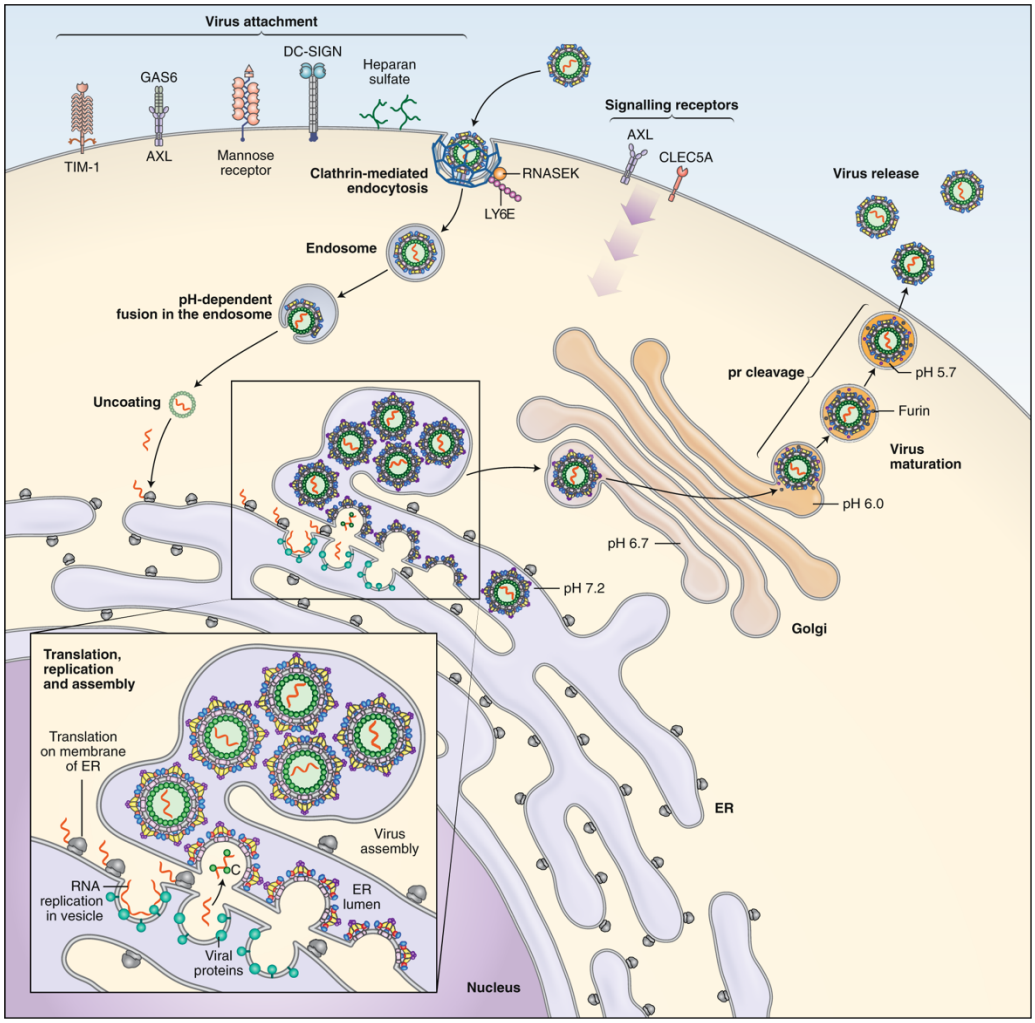

Figure 2. The flavivirus lifecycle within their vertebrate host. Figure sourced from Pierson 2020. Infection is initiated by an infected mosquito vector. Through a series of pH-dependent conformational changes, viral RNA is uncoated, and replication and assembly occurs in the ER and Golgi assisted by a series of viral- and host-encoded proteins**.**

The basic aspects of the flavivirus lifecycle **(Figure 2)** begin when an infected mosquito feeds and introduces virus to the bloodstream. Flaviviruses are capable of binding to a variety of cell types through interactions with extracellular proteins and carbohydrates such as heparan sulfate, dendritic-cell-specific intercellular adhesion molecule-3-grabbing non-integrin (DC-SIGN) and proteins of the TIM and TAM families (Navarro-Sanchez 2003, Meertens 2012). While these host attachment factors are sufficient to initiate infection in a wide variety of cell-types, a bona fide ZIKV or DENV host cell receptor has remained elusive (Perera-Lecoin 2014). Upon attaching to a cell, flaviviruses are internalized via clathrin-dependent endocytic vesicles wherein viral membrane fusion is initiated in a low pH-dependent manner (Chao 2014). Once in the cytoplasm, the viral genome is uncoated and associates with the endoplasmic reticulum (ER) to initiate translation. Replication of the viral genome is then initiated within invaginations of the ER wherein both structural and nonstructural viral proteins encapsulate a genome to form what is referred to as an “immature virion” (Welsch 2009). On the surface of an immature virion, 60 heterotrimeric prM-E spikes undergo a series of conformational changes induced by a locally lower pH in the Golgi – exposing a furin cleavage site found on the E protein. Once exposed, host furin-like serine proteases transform the 60 heterotrimeric prM-E spikes into 90 E dimers. Upon reaching the extracellular space, changes in pH result in the disassociation of M from E and the complete maturation of the virion (Apte-Sengupta 2015). This process of maturation is

both essential for infectivity and has been found to be incomplete in certain cell types and hosts – resulting in morphological variations as well as variability in infectivity (Newton 2021). The *in vivo* relevance of partial maturation is not well known, though studies have shown that this process can affect the antigenic landscape of a virion – impacting the ability of antibodies to bind and neutralize (Maciejewski 2020).

1.3 Antibody-dependent enhancement of flaviviruses

A defining feature of DENV pathogenesis is a phenomenon known as antibody-dependent enhancement (ADE). Though its exact mechanisms remain poorly understood, ADE is broadly described as the enhancement of secondary DENV infection and subsequent disease in the presence of non-neutralizing antibodies. These antibodies are capable of binding to – but not neutralizing – a virion and promoting infection via interactions between antibody Fc regions and host cell Fc-γ receptors. It is postulated that antibodies produced in response to a primary DENV serotype are responsible for ADE when they reach sub-neutralizing quantities and are presented with an infection by a secondary DENV serotype (Halstead 2014). This phenomenon is readily seen with a variety of flavivirus antibodies *in vitro*, but the majority of the evidence for its occurrence *in vivo* result from extensive epidemiological studies on adults as well as infants (Katzelnick 2017, Dejnirattisai 2010, Simmons 2007).

While ADE is primarily understood as occurring between the four DENV serotypes, there is a growing body of literature suggesting that antibodies produced in response to other flaviviruses – particularly ZIKV – may trigger ADE of a secondary DENV infection as well (Anderson 2011, Katzelnick 2020, Bardina 2017). The E proteins of ZIKV and

DENV – a major antigenic site (Dai 2018) – share considerable sequence homology and there is concern that ZIKV may exist alongside DENV1-4 as a member of a larger super serogroup (Barba-Spaeth 2016) and could exacerbate the already challenging ADE dynamic. Given that ZIKV and DENV co-circulate, the development of a broadly neutralizing vaccine for both ZIKV and DENV would be ideal.

1.3 Vaccine efforts and challenges for ZIKV and DENV

While several successful flavivirus vaccines have been developed to date, including a highly effective live-attenuated yellow fever vaccine (YFV-17D) (Collins 2018), efforts to produce a viable vaccine for ZIKV and DENV have been met with variable levels of success. Development of a ZIKV vaccine began in earnest during the 2015-2016 epidemic and as of November 2021, there are 34 completed and 3 in-progress clinical trials listed on ClinicalTrials.gov. A wide variety of vaccine platforms have been utilized including DNA and RNA vaccines, live-attenuated virus, virus-like particles, and inactivated virus (Pattnaik 2020). Recent efforts have been limited largely due to the dramatic decrease in ZIKV infections since the initial outbreak rendering robust clinical trials difficult to complete in addition to a concern for potential adverse outcomes such as ADE as antibody titers wane (Vannice 2019).

DENV vaccine development has a much longer and more complicated history. Currently, there is just one licensed vaccine available for use – Dengvaxia (CYD-TDV). CYD-TDV is a live-attenuated, chimeric vaccine that contains all four DENV serotypes. The backbone of this vaccine is the aforementioned YFV-17D vaccine with the prM and E proteins replaced with that of the four DENV serotypes – resulting in a tetravalent

vaccine. However, this vaccine has been the subject of much controversy over its ability to induce ADE independent of age likely due to imbalanced immune responses to each of the DENV serotypes contained within (Halstead 2017). Additionally, overall efficacy was found to be low – 30.2% (13.4% – 56.6%) – with virtually no efficacy against DENV2 infection (Sabchareon 2012). Currently, this vaccine is only approved for dengue seropositive individuals ages 9 – 45 in dengue-endemic regions for safety reasons which places severe limitations on its use and prevents widespread adoption (Izmirly 2020).

In the absence of safe, effective, and widespread vaccines for ZIKV and DENV, there is a real need for novel approaches to vaccine design. In pursuit of this aim, there have been successful attempts to isolate broadly neutralizing antibodies (bnAbs) capable of neutralizing both ZIKV and DENV with the intention of providing monoclonal antibody therapeutics as well as informing immunogen design for prophylactic interventions. The incredible success of mRNA vaccines encoding for SARS-CoV-2 spike protein highlights the feasibility and potential of this approach for controlling ZIKV and DENV (Polack 2020).

1.4 Broadly neutralizing flavivirus antibodies and epitope mapping

To date, two classes of such bnAbs have been discovered and characterized. The first, known as the E-dimer epitope (EDE) bnAbs were isolated from hospitalized patients in Vietnam who presented with symptomatic DENV infections in 2009 (Dejnirattisai 2015). The second, known as MHRP-Z4 (MZ4) bnAbs were isolated from a ZIKV vaccine trial participant who displayed broad neutralization against ZIKV and DENV in serological assays (Dussupt 2020). It has been postulated that in both cases sequential infection by

ZIKV and DENV allowed for the production of these bnAbs – a claim that is supported by both patient infection history and the antigenic similarity of the E protein for these two viruses. These two bnAb classes target distinct epitopes on the ZIKV and DENV E protein. EDE-class bnAbs – as the name suggests – bind to a conserved quaternary epitope that spans the E dimer **(Figure 3a)** and display potent neutralization of all four DENV serotypes in addition to ZIKV (though with some variability within the class) **(Figure 4a)**. MZ4-class bnAbs bind to a linker region found between domain I and domain III **(Figure 3b)** of the E protein and display potent neutralization of ZIKV, DENV2, and DENV3 with reduced activity against DENV1 and DENV4 **(Figure 4b)**. In general, the existence of these bnAbs represent an exciting opportunity to design an immunogen capable of eliciting a robust, neutralizing response with protective effects against ZIKV and DENV. By better understanding how these bnAbs impart their protective function, it will be possible to present our immune systems with an E protein-based immunogen specifically designed to direct production of cross-protective and safe bnAbs.

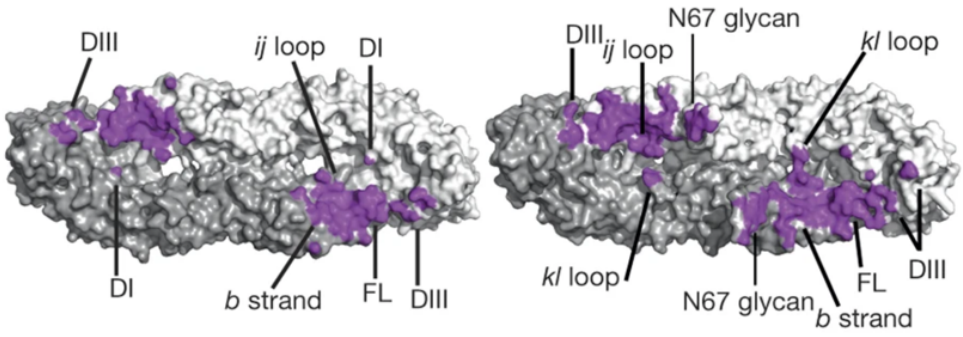

Footprint of EDE1
scFv C8 on ZIKV sE

Footprint of EDE1
Fab C8 on DENV-2 sE

Figure 3a. Footprints of EDE1 C8 – an EDE-class bnAb – on ZIKV and DENV2 E protein dimer. Antibody footprint shown in purple with E monomers colored in light and dark grey with relevant antigenic sites labelled. Figure sourced from Barba-Spaeth 2016.

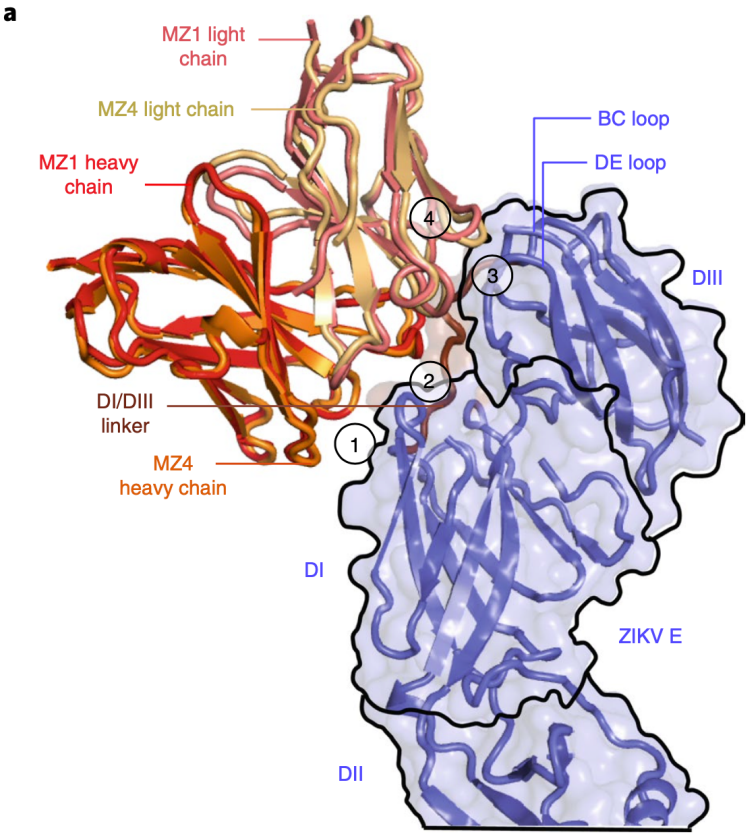

Figure 3b. Superimposition of the crystal structures of MZ4-class bnAbs on ZIKV E protein. MZ1 (red) and MZ4 (orange) variable domains are shown as ribbons with the ZIKV E protein shown in blue. The DI/DIII linker region is highlighted in brown. Figure Sourced from Dussupt 2020.

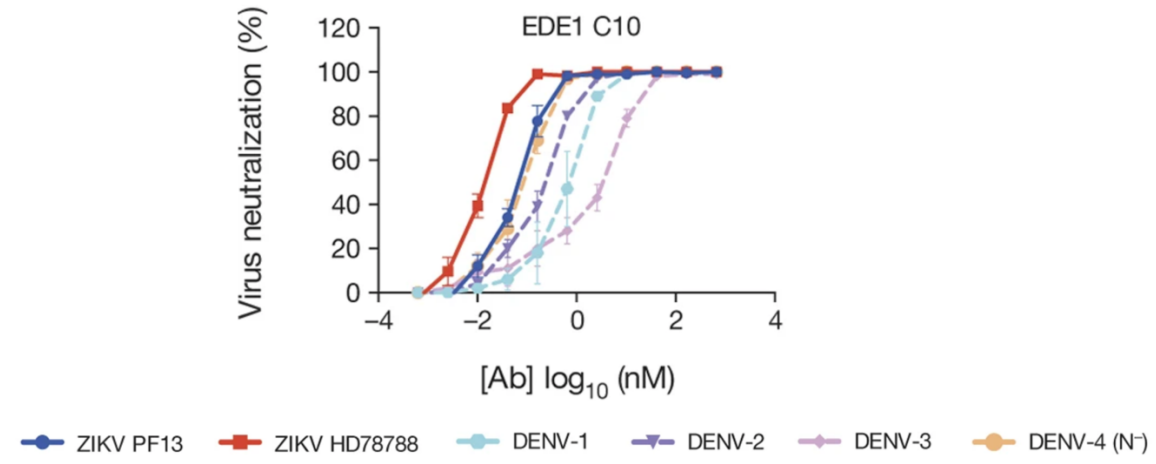

Figure 4a. Neutralization curve for bnAb EDE1 C10 – a representative member of the EDE-class of bnAbs – against DENV1-4 and two strains of ZIKV. EDE1 C10 – like other members of its class – display potent and broad neutralization. Figure sourced from Barba-Spaeth 2016.

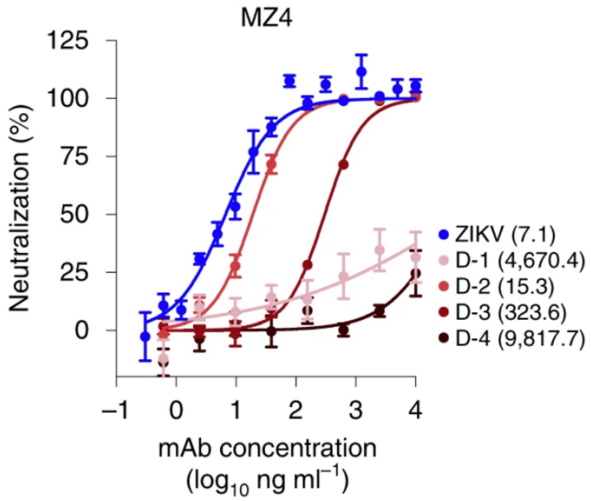

Figure 4b. Neutralization curve for bnAb MZ4 – a representative member of the MZ4-class of bnAbs – against DENV1-4 and two strains of ZIKV. MZ4 displays potent neutralization against ZIKV, DENV2, and DENV3. Figure sourced from Dussupt 2020.

In pursuit of this goal, a variety of epitope mapping methods have been utilized to better understand these bnAbs and how they interact with flavivirus E proteins. These methods, which include alanine scanning, binding competition, shotgun mutagenesis, and x-ray crystallography, provide elegant and informative data on the determinants of

binding, however they are less capable of providing data on *neutralization*. This is an important caveat because of the inherent risks for ADE which, as mentioned, likely results when antibodies are capable of binding to the virion but not neutralizing it. Additionally, previous work on flaviviruses have shown that mutations outside of a structurally defined epitope can have profound effects on neutralization (Goo 2017, Dowd 2015), and current epitope mapping methods either cannot provide that information or require a large amount of serendipity and laborious effort. Regardless, much progress has been made using traditional epitope mapping methods, and we have a growing wealth of knowledge in terms of flavivirus bnAb epitopes. In particular, key amino acid residues have been identified for both classes of bnAbs that mediate binding and neutralization to some degree in addition to revealing information on bnAb dependencies on E protein glycosylation (Barba-Spaeth 2016, Dussupt 2020). In tandem with published data on binding, it is of vital importance to better understand what the determinants of neutralization are for these bnAbs and to do so in a comprehensive, high-throughput manner. Further evidence of this need can be highlighted by a recent attempt to utilize the ZIKV E-dimer as an immunogen (Slon Campos 2019). While this promising approach showed clear protection in mice against challenge by ZIKV, the researchers did not find evidence of cross-reactive bnAbs such as those in the EDE and MZ4 classes. Further investigation of these bnAbs and how they impart their protective function will be useful for the design and implementation of E-dimer immunogens.

1.5 Deep mutational scanning

To better understand the determinants of neutralization for flavivirus bnAbs, I utilized a high throughput and comprehensive epitope mapping approach known as “deep mutational scanning” (DMS). Simply put, DMS involves applying selection pressure to a protein library that contains a large amount of diversity on the amino acid scale. After the selection pressure has been applied, deep sequencing can be used to interrogate the effect of each amino acid mutation by analyzing post-selection sequence abundance. This approach has been used previously to better understand mutation’s effect on the fitness of influenza proteins (Doud 2016), map HIV escape mutations in the presence of HIV bnAbs (Dingens 2017), discover how mutations along the ZIKV E protein affect viral growth (Sourisseau 2019), and even to enrich for ZIKV E protein escape mutations selected by ZIKV-specific monoclonal antibodies (mAbs) (Sourisseau 2019). In this thesis, I will utilize a pre-existing ZIKV E protein DMS library system that was constructed for Sourisseau 2019 and generously shared with us by our collaborators in the Bloom Lab at Fred Hutch. Naturally, identifying escape mutations in a DENV DMS system would also be highly relevant alongside ZIKV, however inherent limitations in cloning techniques for flaviviruses – notably a highly toxic genome in bacteria (Pu 2011) – make the production of such a system challenging in combination with DENV’s lower rescue titers. While efforts to produce such a DENV E protein DMS library are ongoing, this ZIKV DMS library is built on a previously constructed ZIKV infectious clone that was engineered for increased stability in bacteria by incorporating an intron into NS1 – a particularly toxic region of the genome – to increase its genomic stability in bacteria (Schwarz 2016). Additionally, this library has been validated and shown to provide robust antibody

selection data (Sourriseau 2019). My work will be the first time that DMS of flavivirus E protein is used in combination with flavivirus bnAbs. The ZIKV E protein DMS library contains mutations along the ZIKV E protein such that at every amino acid position, there exists all possible substitutions. There are 9,576 total mutations possible within this library considering 19 possible amino acid substitutions at all 504 codons in the ZIKV E protein though a significant portion of these substitutions will result in deleterious effects and may not be functionally relevant. Broadly neutralizing antibodies such as EDE1 C10 and MZ4 can then be mixed with the library and used in a straightforward neutralization assay to select for mutations resulting in antibody escape. Finally, deep sequencing can identify escape mutations that are preferentially enriched within infected cells when compared to infection in the absence of antibody. **Figure 5** contains a schematic overview of the entire workflow.

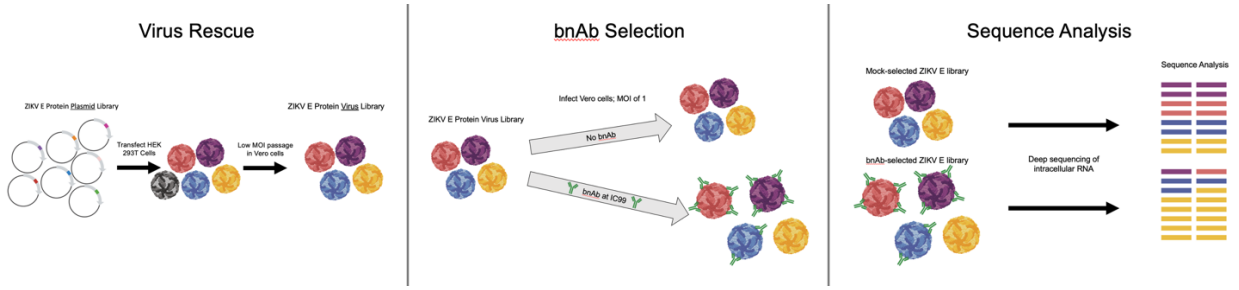

Figure 5. A schematic overview of the workflow included in this thesis. Plasmid is transfected to rescue an intermediary virus library which is then passaged at a low MOI. bnAbs are then used to select for escape mutations which can be identified by sequence analysis of viral transcripts.

Unlike traditional epitope mapping methods which mostly provide information on binding and structural footprints, DMS is a powerful approach because it informs us which

amino acids are responsible for bnAb neutralization and thus provides detailed data on the determinants of neutralization. Another advantage to utilizing a DMS approach is its ability to comprehensively sample all mutations in a single selection experiment – dramatically decreasing the time and effort needed to obtain neutralization data on multiple variants. Once these mutations are identified by deep sequencing, they can then be introduced into a reporter-virus particle system as single mutations to validate their individual functional effects on antibody neutralization.

1.4 Thesis summary

The goal of this thesis is two-fold: 1) to prepare and validate the ZIKV E protein DMS virus library and 2) to use bnAbs EDE1 C10 and MZ4 to apply selective pressure to the ZIKV E protein DMS virus library and identify potential escape mutations. These data will provide information at the amino acid residue level on the determinants of neutralization that, when combined with previously defined structural epitopes, can be used to inform the development of a rational, epitope-based vaccine for both ZIKV and DENV. In Chapter 1, I have introduced ZIKV and DENV and the current status of vaccine development as well as current epitope mapping methods. I have also highlighted two promising classes of bnAbs that target ZIKV and DENV in unique ways and described a powerful epitope mapping approach called DMS. In Chapter 2, I will describe the methods utilized to achieve the above goals as well as the preliminary results of my experiments. I describe the successful rescue of a ZIKV E protein DMS library from plasmid to virus as well as initial attempts to carry out selection assays using bnAbs. I will also report some

limitations on my experiments and ongoing efforts to address them. Chapter 3 will conclude this thesis by discussing my findings, the future directions of this project, as well as some concluding remarks on the implications of my research.

Chapter 2. Defining the determinants of neutralization for broadly cross-reactive flavivirus antibodies

2.1 Introduction

Prior to my arrival, the Goo Lab received plasmids encoding for the ZIKV E protein DMS library (Sourrisseau 2019). These plasmids were then amplified and transfected in biological triplicate to produce an intermediary ZIKV E protein virus DMS library. Subsequently, my first steps were to deep sequence the plasmid library as well as set up a low multiplicity of infection (MOI) passage of the intermediary virus library in order to both purge deleterious mutations and to guarantee a genotype-phenotype link such that the phenotype of each mutant E protein is linked to its genotype within the virion. Once passaged, I deep sequenced the virus library to confirm its diversity and its readiness for use in DMS selection experiments.

For a DMS selection experiment to provide meaningful data, the selection criteria must be very stringent to maximize signal to noise ratio. Therefore, I also sought to identify the concentration of bnAb at which approximately 99% of the virus library is neutralized (IC99). An IC99 will strictly select for only those mutations that result in escape and minimizes the possibility of mutants that do not affect neutralization becoming enriched simply by chance. This way, selected samples can be compared to an unselected sample in order to identify significantly enriched mutations that result in bnAb escape.

Finally, I used bnAb at the identified IC99 to neutralize ZIKV E protein virus library and isolated intracellular RNA to both confirm the neutralization efficiency of the selection assay and as a template for subsequent barcoded-subamplicon deep sequencing. Once

sequenced, the data was analyzed using a software package designed for barcoded-subamplicon deep sequencing (Bloom 2015).

2.2 Methods

Cell lines and culture

HEK 293T/17 cells (ATCC CRL-11268) and Vero C1008 cells (ATCC CRL-1586) were cultured in Dulbecco's modified Eagle's medium (DMEM) (Gibco, catalog #12430054) with 7% fetal bovine serum (FBS) (Gibco, catalog #26140079) and 1% penicillin-streptomycin (Pen-Strep) (Gibco, catalog #15140122). Both cell lines were maintained at 37°C and 5% carbon dioxide (CO_2) and were sub-cultured by first washing with Dulbecco's phosphate-buffered saline (DPBS) (Gibco, catalog #14190144) followed by disassociation using TrypLE Express (Gibco, catalog #12605036) at 37°C until cells were detached. Cells were then either plated for experimental use or a subculture was passaged to continue the line.

Production of ZIKV E protein plasmid library

ZIKV E protein plasmid library was produced using a previously described single-plasmid reverse genetics system for ZIKV strain MR766 as a backbone (Schwarz 2016). Two rounds of mutagenic PCR were performed on ZIKV E protein according to previous methods (Bloom 2014) using a panel of mutagenic primers in addition to primers flanking the E gene. Mutagenized PCR product was cloned into the recipient ZIKV MR766 backbone plasmid using Gibson assembly and then transformed into electrocompetent

Escherichia coli cells (NEB 10-beta) (New England BioLabs, catalog #C3020K) in biological triplicate. Transformants were plated on LB agar supplemented with carbenicillin (100 ug/mL) (TekNova catalog #C8001). Following an overnight incubation at 30°C, all colonies were collected and suspended into 180 mL LB broth using a sterilized glass spreader, then incubated at 30°C for 4 hours. After incubation, plasmid DNA was isolated using a ZymoPURE II Plasmid Maxiprep kit (Zymo Research, catalog #D4203) according to the manufacturer's recommendation.

Rescue of ZIKV E protein virus library

Twenty-four hours prior to transfection, 3 x 6-well tissue culture (TC) plates – one for each plasmid library replicate – were seeded at $1x10^6$ HEK 293T cells per well in 2 mL of low-glucose complete DMEM (Gibco, catalog #12320032) supplemented with 7% FBS and 1% Pen-Strep and incubated at 37°C. On the day of transfection, 1 µg of plasmid DNA per well was transfected using Lipofectamine 3000 reagent (Invitrogen, catalog #L3000015) according to the manufacturer's recommendation. 24 hours post infection, spent media was replaced with fresh media. On day 2 post-transfection, viral supernatant was collected, pooled, filtered (0.45 µm pore size), and stored at -80°C.

Determination of infectious titer of ZIKV E protein mutant library

Twenty-four hours prior to infection, 96-well flat-bottom TC plates (Falcon, catalog #08-772-2C) were seeded at 2 x 10^4 Vero cells per well in 200 µL DMEM (2% FBS and 1% Pen-Strep) and incubated at 37°C. Cells were then infected with 100 µL of serially

diluted virus and incubated at 37°C for 24 hours. Following infection, cells were collected by first washing in DPBS then dissociated using TrypLE Express. Re-suspended cells were then transferred to 96-well V-shaped-bottom plates (Corning, catalog #07-200-96) and pelleted by centrifugation at 300 *x g* for 5 minutes. Titers of rescued virus were determined by immunostaining with the pan-flavivirus E protein-reactive 4G2 antibody conjugated to Alexa Fluor 488 (4G2-AF488) (Novus Biologicals, catalog #NBP2-52666AF488) (1:1500 dilution) using the BD Cytoperm/Cytofix kit (BD Biosciences, catalog #554714) according to the manufacturer's recommendations. Fixed and stained cells were then acquired using the IntelliCyt iQue Advanced Flow Cytometer. Final titers were calculated by averaging the three separate dilution factors according to the following formula:

$$\left[\frac{\left[\left(\frac{4G2\ Positive\ Events}{Total\ Events}\right) \times Total\ Cells\right]}{Volume\ of\ Inoculum\ (mL)}\right] \times Dilution\ Factor = \frac{Infectious\ Units}{mL\ Virus}$$

Low MOI passage of ZIKV E protein virus library

To guarantee a phenotype-genotype linkage and to purge deleterious mutations, 2.5 x 10^7 Vero cells in 150 mL DMEM (2% FBS, 1 % Pen-Strep) were seeded into a Corning 5-chamber CellSTACK culture chamber (Corning, catalog #CLS3319-2EA) 24 hours prior to infection such that there are 5 x 10^7 Vero cells present on the day of infection. Cells were then infected using 1 x 10^6 infectious units of ZIKV E protein virus library which corresponds to an MOI of 0.02. Twenty-four hours following infection, viral inoculum was removed, cells were washed three times using DPBS, and 125 mL of replacement DMEM was added. Forty-eight hours post-infection, 125 mL of replacement

DMEM was again added. Seventy-six hours post-infection, viral supernatant was collected, pooled, filtered (0.45 µm pore size), aliquoted, and stored at -80C.

Identifying an IC99 value by intracellular staining of ZIKV E protein

Twenty-four hours prior to infection, 96-well TC plates were seeded at 2 x 10^4 Vero cells per well in 200 µL DMEM (2% FBS and 1% Pen-Strep) and incubated at 37°C. Threefold serial dilutions of antibody were incubated with 4 x 10^4 IU per well of infectious ZIKV E protein library at 37°C for 1 hour and then transferred to Vero cells for infection in duplicate. Twenty-four hours post infection, cells were harvested, fixed, and stained according to methods outlined above. The percentage of 4G2-AF488-positive cells was then normalized relative to infected cells in the absence of antibody and an IC99 value was calculated according to GraphPad Prism's built-in features (GraphPad).

Determining neutralization by ZIKV RT-qPCR

Twenty-four hours prior to infection, 6-well TC plates were seeded at 4 x 10^5 Vero cells per well in 2 mL DMEM (2% FBS and 1% Pen-Strep) and incubated at 37°C. Serial dilutions of antibody were incubated with 8 x 10^5 IU per well of infectious ZIKV E protein library at 37°C for 1 hour and then transferred to Vero cells for infection. Twenty-four hours post-infection, cells were washed twice with DPBS, detached using TrypLE Express, re-suspended in DMEM, and centrifuged at 300 *x g* for 5 minutes. Intracellular RNA was then isolated using the QIAGEN RNeasy Plus Mini kit (Qiagen, catalog #74134) according to the manufacturer's recommendations for adherent mammalian cells. 2 µL of

RNA from each sample was diluted 1:10 prior to quantifying using a Nanodrop spectrophotometer set to determine RNA yield and purity.

Isolated RNA was then normalized to 20 or 40 ng of total RNA and viral RNA was quantified by ZIKV-specific qRT-PCR using a qScript One-Step SYBR Green RT-qPCR Low Rox kit (VWR, catalog #95054-954) as previously described (Sourisseau 2019). See **Table 1** for primer sequences. To produce a standard curve of viral RNA copies, *in vitro*-transcribed ZIKV MR766 RNA was produced using a MEGAscript T7 transcription kit (Invitrogen, catalog #AM1334) according to the manufacturer's recommendation and aliquoted at 100 ng/uL (1.16×10^{11} RNA copies/uL). Standard curve RNA was then prepared for RT-qPCR by first diluting 6 uL of RNA into 342 uL nuclease-free water to produce a 2×10^9 RNA copies/uL solution. Then, a 10-fold serial dilution was performed and 5 uL of each standard was used in the final reaction.

Selection of antibody escape mutants

Twenty-four hours prior to infection, 6-well TC plates were seeded at 4×10^5 Vero cells per well in 2 mL DMEM (2% FBS and 1% Pen-Strep) and incubated at 37°C. On the day of infection, 800 uL of bnAb EDE1 C10 (at two concentrations – 400 and 300 ng/mL) were incubated with ZIKV E protein library at an MOI of 1 at 37°C for 1 hour and then transferred to Vero cells for infection. Twenty-four hours post-infection, cells were washed twice with DPBS, harvested using TrypLE, and intracellular RNA was isolated as described above for subsequent barcoded-subamplicon deep sequencing.

Barcoded-subamplicon deep sequencing

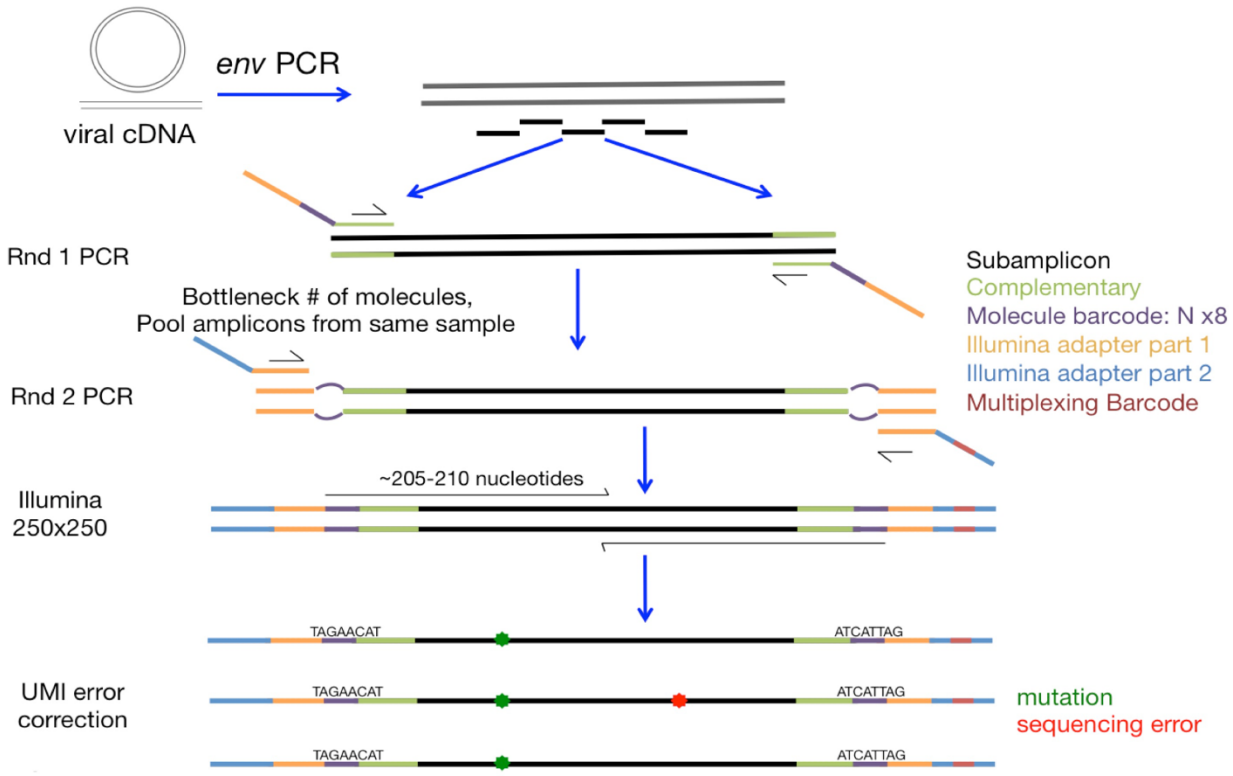

Figure 6. Schematic overview of barcoded-subamplicon deep sequencing. Figure sourced from Dingens 2017. Full length ZIKV E gene is broken up into 5 subamplicons that then have Illumina adapters and UMIs incorporated through a series of PCR steps. This deep sequencing approach allows for robust error correction.

Barcoded-subamplicon deep sequencing was performed as previously described (Sourisseau 2019) and is outlined in **Figure 6**. Briefly, reverse-transcription of 1000 ng total isolated RNA was carried out for each sample using an AccuScript High-Fidelity Reverse Transcriptase kit (Agilent, catalog #200820) and ZIKV-specific primers flanking the E-gene (see **Table 1** for primer sequences). The full-length E coding sequence was then amplified (PCR1) using a KOD Hot Start DNA polymerase kit (KOD HS) (Sigma-

Aldrich, catalog #71842-3) according to the manufacturer's protocol. Five subamplicons spanning the full length of the E coding sequence were then generated (PCR2) (see **Table 1** for primer sequences) using a KOD HS kit on 4 ng of PCR product from the previous step. These primers also add an N8 randomized barcode as well as Illumina adapter sequences. The thermal cycling conditions are as follows:

Step Number	**Temperature (°C)**	**Duration**
1	95	2 Minutes
2	95	20 Seconds
3	70	1 Second
4	50 (0.5°C/second)	20 Seconds
5	70	20 Seconds
6	Repeat Steps 2-5 for 10 cycles total	
7	95	1 Minute

Following amplification, all subamplicons were purified by AMPure XP beads (Beckman Coulter, catalog #A63880) at a 1:1 bead to sample ratio and 7.5 x 10^5 DNA molecules of each subamplicon were pooled by sample. DNA was quantified via Qubit dsDNA HS assay (Invitrogen, catalog #Q33230).

A KOD HS kit was used for PCR3 which utilizes primers that are complementary to the Illumina adapter sequence in PCR2 and add the second Illumina adapter sequence in addition to a NEXTflex multiplexing barcode (see **Table 1** for primer sequences). The thermal cycling conditions are as follows:

Step Number	**Temperature (°C)**	**Duration**

1	95	2 Minutes
2	95	20 Seconds
3	70	1 Second
4	55 (0.5°C/second)	20 Seconds
5	70	20 Seconds
6	Repeat Steps 2-5 for 24 cycles total	

The resulting PCR products were then purified by AMPure XP beads (1:1 ratio) and quantified using a Qubit 1X dsDNA HS kit. Finally, 500 ng of each sample was pooled, and run on a SYBR Safe (Invitrogen, catalog #S33102) 1% UltraPure agarose gel (Invitrogen, catalog #16500100) at 70V for 50 minutes. DNA of the appropriate size – approximately 500 base pairs – was extracted using a QIAquick Gel Extraction kit (Qiagen, catalog #28704), purified by AMPure XP beads (1:1 ratio), and quantified via Qubit dsDNA HS assay. Subamplicons were submitted at 2 nM and sequenced on either an Illumina MiSeq using 2 x 250 paired-end reads with 15% Phi-X spiked in.

Analysis of deep sequencing data

All data analysis of deep sequencing data generated by these experiments was performed by either Jesse Bloom or Caroline Kikawa. All computer code used in the analysis can be found at https://github.com/jbloomlab/dms_tools2, the notebook containing analyzed data from the library generation can be found at https://github.com/jbloomlab/ZIKV_MAP_GooLab, and the notebook containing

analyzed data from the EDE1 C10 selections can be found at https://github.com/ckikawa/Goo-lab-C10-NOV21/blob/main/CK_analysis_nbook.ipynb.

Briefly, dms_tools2 (Bloom 2015) was used to identify the occurrence of every mutation in each sample. The amino acid preferences at each site were then computed using these sites by dividing the log of the preference value of the mutation divided by the preference value for the WT amino acid.

Primer Name	Primer Sequence	Primer Purpose
Primer_1	TTGGTCATGATACTGCTGATTGC	ZIKV-specific forward primer for RT-qPCR
Primer_2	CCYTCCACRAAGTCYCTATTGC	ZIKV-specific reverse primer for RT-qPCR
Primer_3	GCCATTGCCTGGCTTTTGGGAAGC	Forward primer for full-length ZIKV E gene (PCR1)
Primer_4	TGGTACTTGTACCGGTCCCTCCAGGC	Reverse primer for full-length ZIKV E gene (PCR1)
Primer_5	CTTTCCCTACACGACGCTCTTCCGATCT NNNNNNNNCTGCTGATTGCCCCGGCAT ACAGT	Forward primer for subamplicon 1 (PCR2)
Primer_6	GGAGTTCAGACGTGTGCTCTTCCGATC TNNNNNNNNCCTTTGCCAAAAAGTCCA CAACCGTTTCC	Reverse primer for subamplicon 1 (PCR2)

Primer_7	CTTTCCCTACACGACGCTCTTCCGATCT NNNNNNNNGCAAAAGAACATTAGTGGA CAGAGGTTGG	Forward primer for subamplicon 2 (PCR2)
Primer_8	GGAGTTCAGACGTGTGCTCTTCCGATC TNNNNNNNNGCACCAACCAATGCTTATT GTTCATGGTCAG	Reverse primer for subamplicon 2 (PCR2)
Primer_9	CTTTCCCTACACGACGCTCTTCCGATCT NNNNNNNNGGACAGGCCTTGACTTTTC AGATCTGTATTAC	Forward primer for subamplicon 3 (PCR2)
Primer_10	GGAGTTCAGACGTGTGCTCTTCCGATC TNNNNNNNNCGCAGTGCACAAGGAATA TGACACGCC	Reverse primer for subamplicon 3 (PCR2)
Primer_11	CTTTCCCTACACGACGCTCTTCCGATCT NNNNNNNNGCCGCCTAAAAATGGACAA GCTTAGATTGAAG	Forward primer for subamplicon 4 (PCR2)
Primer_12	GGAGTTCAGACGTGTGCTCTTCCGATC TNNNNNNNNCCTTTCCGATGGTGCTAC CACTCCTATG	Reverse primer for subamplicon 4 (PCR2)
Primer_13	CTTTCCCTACACGACGCTCTTCCGATCT NNNNNNNNGGGGACAAGAAAATCACCC ACCACTGG	Forward primer for subamplicon 5 (PCR2)
Primer_14	GGAGTTCAGACGTGTGCTCTTCCGATC TNNNNNNNNGAGAAGTCCACTGAGCAC CCCACATC	Reverse primer for subamplicon 5 (PCR2)
Primer_15	AATGATACGGCGACCACCGAGATCTAC ACTCTTTCCCTACACGACGCTCTTCCGA TCT	Universal multiplexing forward primer (PCR3)
Primer_16	CAAGCAGAAGACGGCATACGAGATATC ACGTTGTGACTGGAGTTCAGACGTGTG CTCTTCCGATCT	Multiplexing reverse primer (PCR3)
Primer_17	CAAGCAGAAGACGGCATACGAGATCGA TGTTTGTGACTGGAGTTCAGACGTGTG CTCTTCCGATCT	Multiplexing reverse primer (PCR3)

Primer_18	CAAGCAGAAGACGGCATACGAGATTTA GGCATGTGACTGGAGTTCAGACGTGTG CTCTTCCGATCT	Multiplexing reverse primer (PCR3)

Table 1. Primer names, sequences, and role in this thesis.

2.3 Results

Rescued ZIKV E protein virus library achieves high titer

To prepare ZIKV E protein virus library for use in subsequent DMS selection experiments, our group received plasmids encoding for the virus library from our collaborators in the Bloom Lab at Fred Hutch. This plasmid system was first constructed and published in Sourisseau 2019. Our group then amplified these plasmids through transformation of NEB 10-beta *E. coli* cells. After amplifying the plasmids, the workflow outlined in **Figure 6** was followed in biological triplicate. Following transfection, the intermediary virus library produced titers of 1.1 x 10^6 IU/mL, 5 x 10^5 IU/mL, and 1.1 x 10^6 IU/mL for each replicate. Wild-type ZIKV was also included as a useful transfection control and achieved a titer of 3.9 x 10^6 IU/mL. These were then passaged at a low MOI (0.02) in order to purge deleterious mutations as well as guarantee a genotype-phenotype link. This step is crucial because during the construction of the plasmid library by overlapping PCR mutagenesis all mutations regardless of their effect are incorporated into the library. A significant number of these mutations will encode for nonsynonymous mutations that either directly encode for deleterious stop codons or mutations that result in E proteins that are incapable of continuing infection. Additionally, during the transfection step, there is the possibility that multiple plasmids are transfected into a single cell and as a result

may produce virions that are phenotypically distinct from their packaged genomes. A low MOI passage addresses both of these concerns as well as allows us to produce large volumes of virus for use in numerous selection experiments. Virus supernatant was collected and filtered on day 3 post-infection and titrated. The titers from the low MOI passage are: 1.1 x 10^6 IU/mL for library 1, 1.0 x 10^6 IU/mL for library 2, 1.1 x 10^6 IU/mL for library 3, and 2.6 x 10^6 IU/mL for WT.

To confirm the presence of sufficient genetic diversity in the virus libraries, and to verify that deleterious mutations had been purged, barcoded-subamplicon deep sequencing was performed. As shown in **Figure 7**, deleterious stop mutations that were present in the plasmid libraries were indeed purged during the low MOI passage and that roughly half of the mutations are no longer seen in the virus library. **Figure 7** also **highlights** the marginal rate of mutation in the wild-type plasmid and wild-type virus samples – suggesting that polymerase and sequencing errors are not contributing to the genetic diversity seen in our sequencing data.

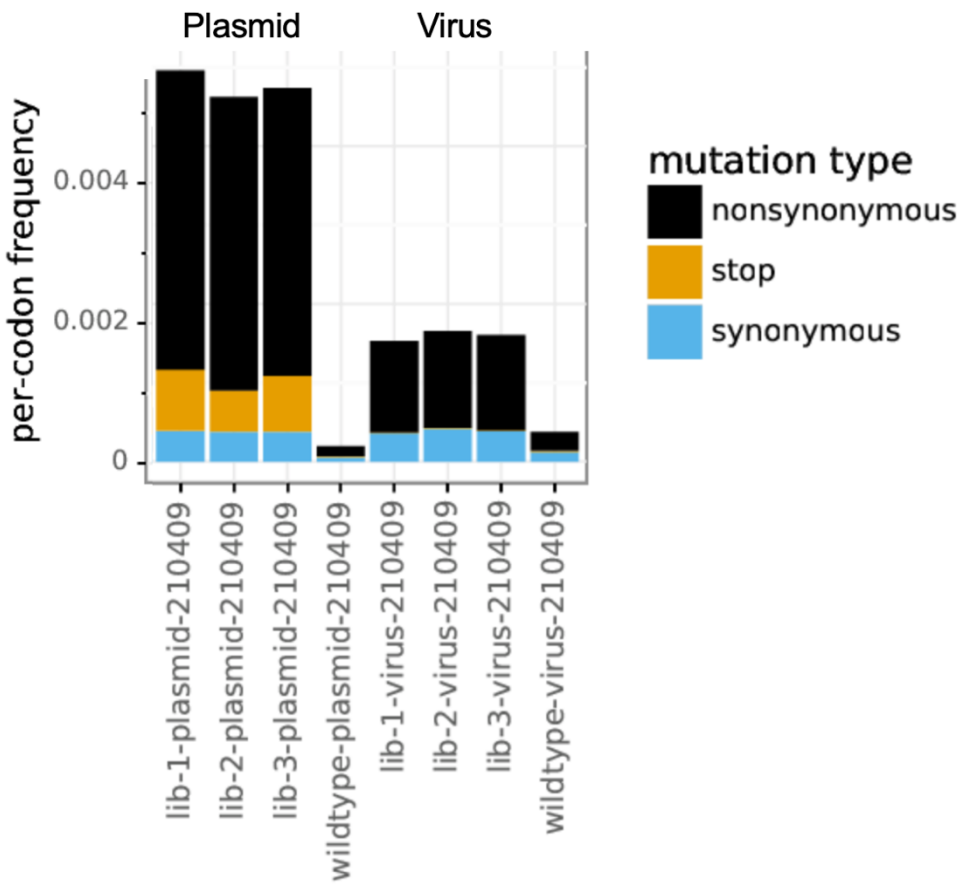

Figure 7. Mutation frequency per codon of ZIKV E plasmid libraries and ZIKV E virus libraries in biological triplicate. Following transfection and a low MOI passage, stop codons and other deleterious mutations are purged from the virus library. Wild-type plasmid and virus contain significantly fewer mutations than the libraries as expected.

While the titers and mutational frequencies of the library are in line with previously published data (Sourisseau 2019), this step represents a potential limitation of a DMS approach. Sites along the E protein that are mutationally tolerant will by definition allow for more nonsynonymous mutations at that site while more conserved regions – the natural target of bnAbs – will be less tolerant and therefore have fewer mutations present in the virus library. One could theorize that this reduction in diversity specifically at conserved sites may result in challenges when exploring enriched sequences selected by bnAbs as we will see later. Given that limitation, however, analysis of the deep

sequencing data supports the conclusion that the rescue of a ZIKV E protein virus library was successful and matches previously reported data (Sourisseau 2019). These libraries are ready for use in ensuing DMS experiments.

Identification of an IC99 value for bnAbs EDE1 C10 and MZ4

When performing a DMS experiment, it is necessary to impart a stringent selection criterion on the virus library to obtain a clear selection signal distinct from the underlying noise. Without a strong selection pressure, mutations that have no effect on antibody escape will be abundant and will contribute to potential background noise when interpreting enriched mutations. Therefore, it is necessary to use bnAb at a high concentration in order to select for genuine escape mutations. To accomplish this, an antibody inhibitory concentration of approximately 99% (IC99) was identified such that 99% of the virus library is neutralized.

To begin, and to preserve reagents associated with RT-qPCR-based neutralization assays, I utilized a broad range of concentrations for both EDE1 C10 and MZ4 and performed intracellular staining of ZIKV E protein to determine a preliminary % neutralization at each concentration in technical triplicate **(Figure 8)**. EDE1 C10 ranged from 2380 ng/mL to 9.3 ng/mL in two-fold dilutions while MZ4 ranged from 2520 ng/mL to 9.8 ng/mL in two-fold dilutions; these concentrations were informed by previously reported data on these bnAb's activity against ZIKV (Barba-Spaeth 2016, Dussupt 2020). Of note, these IC99 identification assays were carried out on wild-type ZIKV and likely underestimate the necessary quantities of bnAb needed to neutralize an equivalent MOI of ZIKV virus library. After averaging the % neutralization at each concentration, I

identified the two concentrations that resulted in neutralization closest to 99% - 150 and 74 ng/mL for EDE1 C10, and 1260 and 630 ng/mL for MZ4.

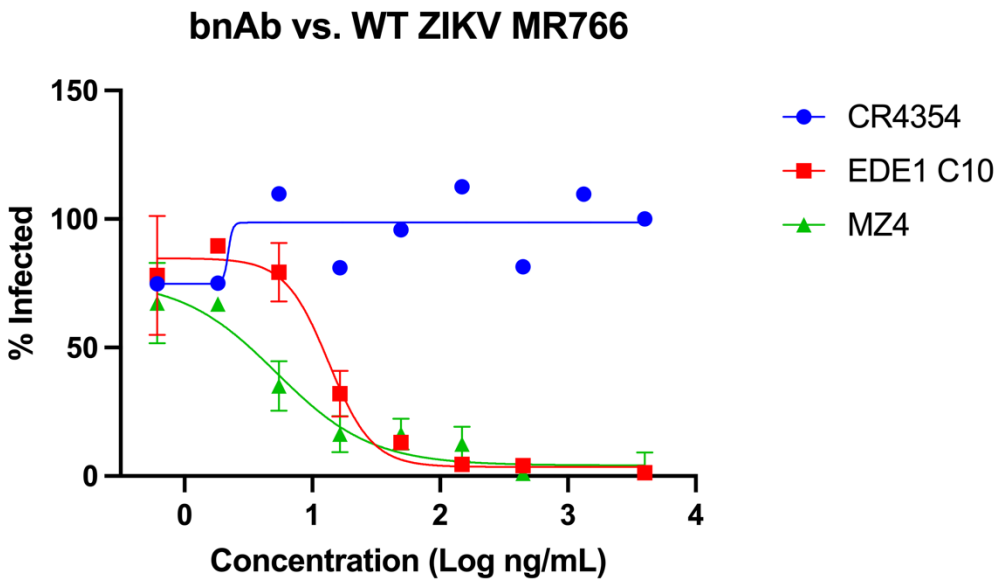

Figure 8. Neutralization curve for bnAbs EDE1 C10 and MZ4 against WT ZIKV. EDE1 C10 (red) and MZ4 (green) robustly neutralize WT ZIKV. While EDE1 C10 has clearly defined upper and lower limits (0 and 100% neutralization), MZ4 consistently lacked an upper plateau. CR4354 (blue) is a West Nile virus-specific mAb that does not neutralize ZIKV and acts as a control. Figure is of one representative replicate.

As these intracellular staining assays were performed in 24-well format (to conserve reagent) and the eventual DMS experiments are performed in 6-well format, I then used these IC99 values in a 6-well format to verify their accuracy both in that format, but also when determining neutralization by RT-qPCR. RT-qPCR – being based on the analysis of viral RNA transcripts – is a more relevant assay for DMS experiments. As is expected when alternating experimental format and assay, there were slight adjustments made to bnAb concentration in order to maintain 99% neutralization. Notably, EDE1 C10

required 300 ng/mL to achieve an IC99 while MZ4 achieved an IC99 at the previously determined 1260 ng/mL.

Selection of bnAb escape mutants and deep sequencing of enriched mutations

Upon identifying an IC99 value for bnAbs EDE1 C10 and MZ4, selections of bnAb escape mutants could be performed using the ZIKV E protein virus library. Virus library and bnAb were incubated and used to infect cells for 24 hours prior to isolating intracellular RNA and performing barcoded-subamplicon deep sequencing. Isolated RNA from the selection experiment was also used to perform RT-qPCR and confirm neutralization %. While EDE1 C10 displayed robust neutralization at 400 ng/mL and 300 ng/mL (99.6% and 98.5% respectively), MZ4 surprisingly experienced a dramatic reduction in neutralization – even at 2000 ng/mL (21.2%). This significant decrease in neutralization was not expected and either represents an experimental issue that can be resolved by repeating the experiment, or possibly a biological phenomenon due to the nature of the virus library. As mentioned, IC99 was determined against WT ZIKV, not the virus library. It is therefore possible that MZ4 has inherent limitations when neutralizing a genetically diverse virus library compared to WT. In either case, poor neutralization is an indicator that subsequent sequencing will not be able to identify significantly enriched mutations and sequencing MZ4 was not prioritized at this time. As EDE1 C10 continued to neutralize the virus library at close to 99%, I continued with deep sequencing these samples. The decision to include both EDE1 C10 concentrations in sequencing was made so as to maximize the likelihood of identifying significantly enriched mutations.

Analysis of the barcoded-subamplicon deep sequencing data was performed and showed both successes and room for troubleshooting. From a technical standpoint, the sequencing worked well. In order to avoid potential PCR bias, subamplicons were bottlenecked to 1.5 x 10^6 barcodes per sample prior to further amplification, and deep sequence analysis showed that this target was indeed achieved **Figure 9** with the majority being aligned. In order to properly error correct based off barcode sequences, and to account for inefficiencies in deep sequencing, I aimed for each barcode to be read 4 times which would correspond to 6 x 10^6 reads per sample. **Figure 9** also shows that this was successful in terms of total reads.

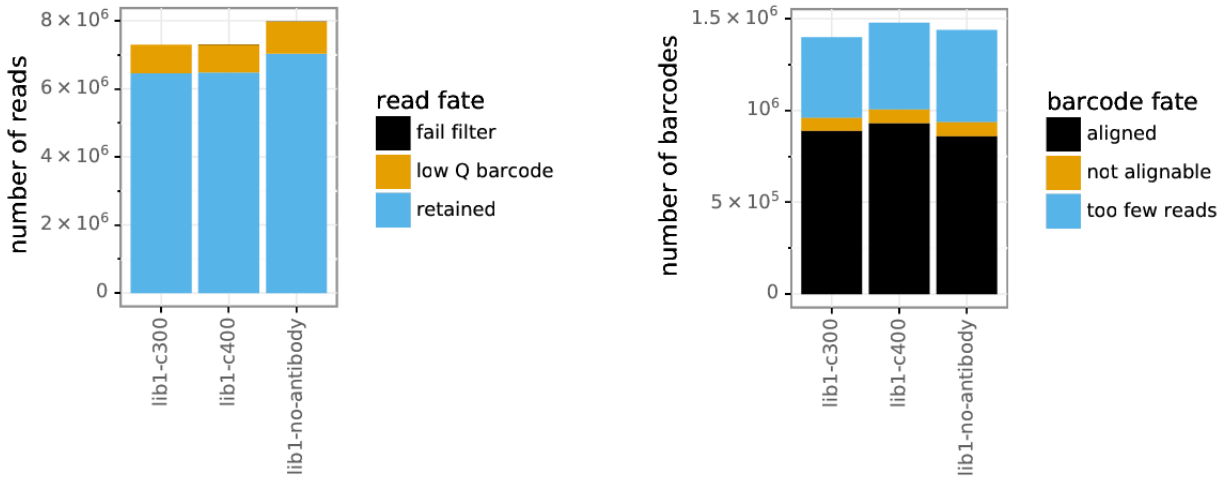

Figure 9. Deep sequencing data showing the number of reads and number of barcodes per sample – C10 at 300 ng/mL, C10 at 400 ng/mL, and unselected virus library. Nearly 1 x 10^6 barcodes per sample were aligned for error correcting with a total of approximately 6 x 10^6 reads per sample.

However, when looking at the number of times each barcode was sequenced **(Figure 10)**, there are far more barcodes being read once (and therefore incapable of being error corrected) than expected. While this potentially limits the number of enriched mutations

capable of being identified, the majority of barcodes were indeed read two or more times and could be used to error correct.

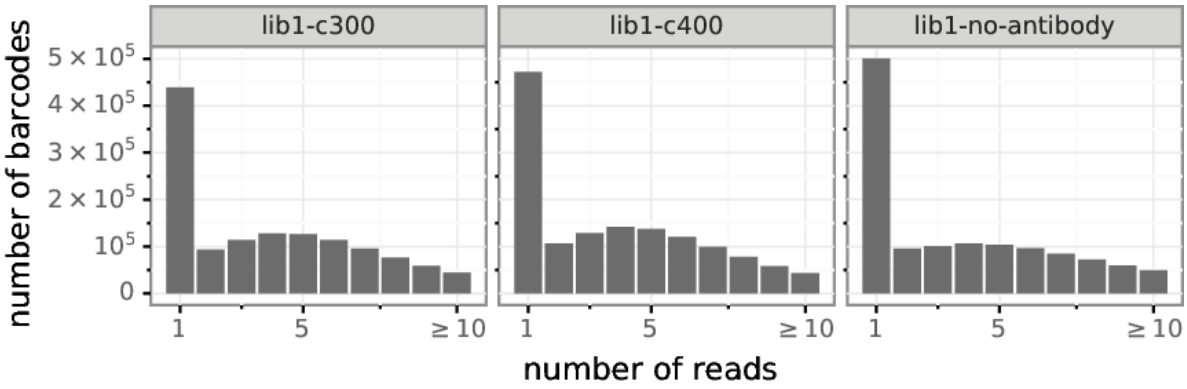

Figure 10. Number of times each barcode was read. To correct for sequencing errors, a barcode must be read at least twice. While many barcodes are read only once, the majority are able to be error corrected.

Prior work using EDE1 C8 – a highly related bnAb to EDE1 C10 – revealed which amino acid residues on ZIKV E protein are responsible for antibody binding (Barba-Spaeth 2016). While binding and neutralization do not always correlate (Durham 2019), we theorized that some portion of these residues will be involved in neutralization. However, when examining the mutations that were enriched by EDE1 C10 selection **(Figure 11)**, it becomes clear that a more stringent selection pressure must be applied.

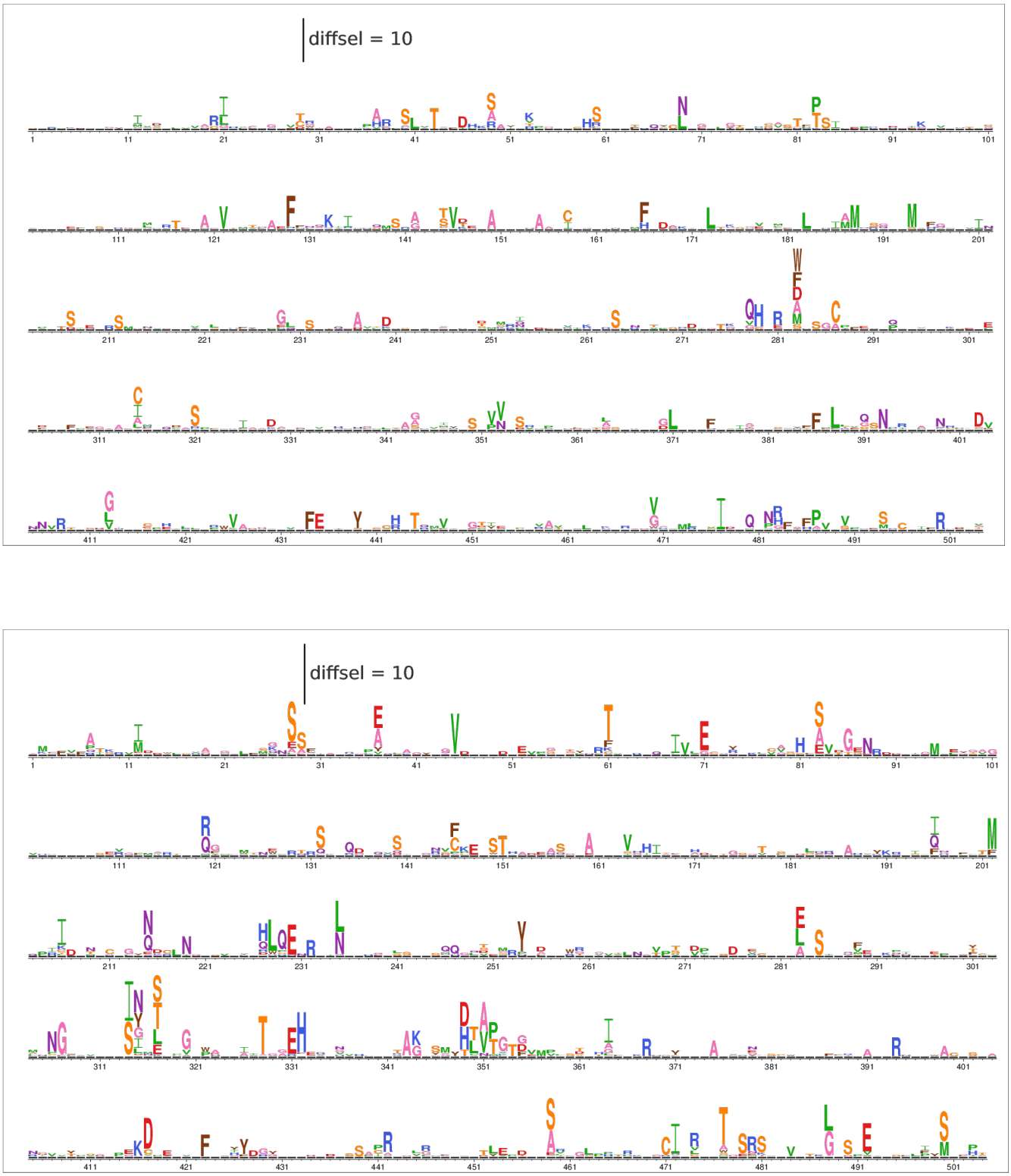

Figure 11. EDE1 C10-selected mutations at each position along the ZIKV E protein when selected by 300 ng/mL (top) and 400 ng/mL (bottom) of bnAb. The lack of clear selection signal at previously known binding sites in addition to very little consistency between samples suggests that a stricter selection pressure needs to be applied.

When comparing the epitope identified in Barba-Spaeth 2016 to the residues identified here, there are two things that stand out: 1) the residues that show the most significant amount of enrichment (identified by the relative size of the font) have no overlap with the known EDE1 C10 epitope and are not consistent across both experimental replicates, and 2) the residues involved with EDE1 C8 binding do not show significant selection by DMS at either C10 concentration. Both observations suggest that insufficient selection pressure was applied to the virus library as to separate signal from noise. If this assumption is correct, increasing the concentration of bnAb and neutralizing more of the virus library should result in clearer data. Additionally, as this ZIKV E protein DMS library has been utilized in the past to identify escape mutations against ZIKV-specific mAb ZKA64 (Sourisseau 2019), we are preparing the selections using ZKA64 in order to verify that our approach is able to recapitulate their findings and to validate our workflow. Also worth considering, as briefly mentioned before, epitopes of bnAbs tend to be focused on highly conserved amino acids that could reasonably be assumed to have a reduced tolerance for mutation. If this is the case, the low MOI passage of the intermediary virus library may have purged these mutations. Further analysis of the deep sequencing data will be able to address this concern by confirming the presence or absence of genetic diversity at these residues in the virus library.

Chapter 3. Discussion and Future Directions

3.1 Discussion

In the previous chapter, I described the successful rescue of a ZIKV E protein virus library capable of being used in DMS experiments to investigate escape mutations selected for by myriad selection pressures. I then utilized this virus library to interrogate the effects of individual mutation in ZIKV E protein on escape from bnAbs EDE1 C10 and MZ4 – members of the two known classes of antibodies capable of neutralizing both ZIKV and DENV. Ultimately, the selection failed to identify significantly enriched mutations, but the barcoded-subamplicon deep sequencing was technically successful.

When rescuing the virus library, a primary concern was maintaining genetic diversity while achieving high titers and purging any deleterious mutations. To achieve this, we collected intermediary virus following transfection at an early time point to prevent repeated infection of the transfection cells. HEK 293T cells are permissive to ZIKV infection and there is the risk that certain genomes may become overrepresented in the library if unexpected rounds of replication were to occur. After transfection, a very low MOI passage was conducted primarily to select against mutations that result in a severe loss of fitness. Should these mutations not be purged and included in the antibody selection experiment, they would be incapable of infection and therefore their genome would not be able to be sequenced regardless of their effect on antibody escape. Additionally, an advantage of this DMS approach is the use of fully infectious ZIKV so genomes that do not encode for infectious virus should be excluded. Another benefit of the low MOI passage is guaranteeing a linked genotype and phenotype. Transfection can

introduce multiple genomes into a single cell and there is a possibility that a mismatched genome can then become packaged into the inappropriate virion. As DMS relies on associating a single point mutation with its phenotypic effect, this mismatch would result in improper conclusions during sequence analysis. A low MOI passage all but guarantees only one virion infects any given cell – preventing a mismatch. Deep sequencing of the virus library – produced in biological triplicate – confirmed both the library's genetic diversity as well the lack of deleterious mutations.

In order to use this library to discover bnAb escape mutations, I identified an IC99 value for EDE1 C10 and MZ4. Initially, I used a broad range of bnAb concentrations and intracellular staining for E protein to identify promising concentrations. While this approach was successful in identifying concentrations that resulted in greater than 99% neutralization, there were some challenges associated with adjusting the experiment format (24-well to 6-well, for example) as well as the assay used to determine % neutralization. To verify successful neutralization of the virus library in the actual selection experiments, I perform RT-qPCR on isolated RNA prior to reverse-transcribing to produce cDNA for deep sequencing. Therefore, I wanted to confirm my IC99 values using this assay. In general, IC99 values were consistent across the two assays, but EDE1 C10 in particular required some adjustments to its concentration. Originally, I determined IC99 values against wild-type ZIKV, but discovered these values were not particularly accurate against the actual virus library. MZ4 experienced a significant reduction in neutralization and further experiments will likely need to be conducted to identify a new IC99 value against the virus library. EDE1 C10 mostly maintained its neutralization and I was able to continue with the selection using two concentrations of bnAb.

Initially, I ran into some technical challenges with the barcoded-subamplicon deep sequencing. In particular, I consistently saw imbalanced subamplicon barcodes. The five subamplicons that make up the full ZIKV E gene should be mixed at equal amounts prior to PCR3 and therefore the number of barcodes for each subamplicon should also be equal. Yet I repeatedly saw fewer barcodes in subamplicon 2, 3, and 5. Luckily, the fix was quite simple – ordering new primers. A more technically challenging problem that still remains to some degree is how many times an individual barcode gets read. In order to accurately correct for sequencing errors, each barcode must be read at least twice, however the vast majority of my barcodes were not being read more than once. To address this issue, I reduced the number of barcodes going into PCR3 to prevent any potential PCR bias, and I dedicated more reads of each Illumina run to my samples. While this did significantly increase the number of barcodes being read twice or more, there are still an unexpectedly large number of barcodes only being read once. Unfortunately, if a barcode is only read once, the sequence does not get included in the analysis and potential escape mutations could go unnoticed. Improving this aspect of the sequencing may also improve selection data.

While my initial attempt at identifying significantly enriched mutations was not successful for reasons discussed in Chapter 2, there is a clear path forwards for troubleshooting this experiment. First, the RT-qPCR assay suffers from technical variation that can result in a log-fold difference in viral RNA copies. This variation could be preventing an accurate % neutralization from being determined which could explain the lack of selection signal. If the library is in fact being neutralized far less than expected, there would be too much background noise to identify significant mutations. Additionally,

I performed the selection assay using mAb ZKA64 which has previously had its epitope defined by DMS which will be a highly useful sequencing control. Should this selection recapitulate the previous findings, then we can be confident in our workflow.

In all, the successful work conducted in this thesis has prepared for future experiments and opportunities using this ZIKV E protein virus library.

3.2 Future directions

With virus in hand, there are many routes of inquiry available. First, and foremost, significantly enriched mutations will need to be validated by introducing individual mutations into a ZIKV reporter virus particle (RVP) system and measuring its impact on neutralization. This step is essential for concluding that individual mutations are responsible for antibody escape and not simply an experimental artefact or some other biologically irrelevant explanation. From there, I would be particularly interested in introducing EDE1 C10 escape mutations into a DENV RVP system to better understand which residues contribute to C10's broad reactivity.

Preliminary efforts have been made in our lab to use the ZIKV E protein virus library to investigate polyclonal responses found in broadly neutralizing sera. It will be fascinating to explore the similarities and differences in the epitopes targeted by known bnAbs and broadly neutralizing sera. In a similar line of thought, our lab is using single cell approaches to identify more classes of flavivirus bnAbs, and the virus library could very well be used to map those novel epitopes.

3.4 Conclusion

Through the work described in this thesis, I have rescued ZIKV E protein virus library capable of being used in DMS approaches. In pursuit of better understanding the determinants of neutralization for antibodies that are broadly protective against ZIKV and DENV, I identified an IC99 value for bnAbs EDE1 C10 and MZ4 – members of the two known classes of flavivirus bnAbs. I then sought to select for bnAb escape mutants using the ZIKV E protein virus library by barcoded-subamplicon deep sequencing intracellular RNA of bnAb-selected samples. While technical aspects of deep sequencing were successful, my initial efforts failed to identify significantly enriched mutations. Regardless, this thesis has laid the groundwork for a plethora of future experiments designed to reveal the determinants of neutralization for bnAbs and more.

References

Aktepe TE, Mackenzie JM. Shaping the flavivirus replication complex: It is curvaceous!. Cell Microbiol. 2018;20(8):e12884. doi:10.1111/cmi.12884

Anderson KB, Gibbons RV, Thomas SJ, et al. Preexisting Japanese encephalitis virus neutralizing antibodies and increased symptomatic dengue illness in a school-based cohort in Thailand. PLoS Negl Trop Dis. 2011;5(10):e1311. doi:10.1371/journal.pntd.0001311

Apte-Sengupta S, Sirohi D, Kuhn RJ. Coupling of replication and assembly in flaviviruses. Curr Opin Virol. 2014 Dec;9:134-42. doi: 10.1016/j.coviro.2014.09.020. Epub 2014 Oct 18. PMID: 25462445; PMCID: PMC4268268.

Bäck AT, Lundkvist A. Dengue viruses - an overview. Infect Ecol Epidemiol. 2013;3:10.3402/iee.v3i0.19839. Published 2013 Aug 30. doi:10.3402/iee.v3i0.19839

Barba-Spaeth, G., Dejnirattisai, W., Rouvinski, A. et al. Structural basis of potent Zika–dengue virus antibody cross-neutralization. Nature 536, 48–53 (2016).

https://doi.org/10.1038/nature18938

Bardina, S.V., Bunduc, P., Tripathi, S., et al. Enhancement of Zika virus pathogenesis by preexisting antiflavivirus immunity. Science 356(6334): 175-180 (2017). DOI: 10.1126/science.aal4365

Bhatt, S., Gething, P., Brady, O. et al. The global distribution and burden of dengue. Nature 496, 504–507 (2013). https://doi.org/10.1038/nature12060

Bloom JD. 2014. An experimentally determined evolutionary model dramatically improves phylogenetic fit. Mol Biol Evol 31:1956–1978. https://doi.org/10.1093/molbev/msu173.

Bloom JD. 2015. Software for the analysis and visualization of deep mutational scanning data. BMC Bioinformatics 16:168. https://doi.org/ 10.1186/s12859-015-0590-4.

Burke, D. S., Nisalak, A., Johnson, D. E. & Scott, R. M. A prospective study of dengue infections in Bangkok. Am. J. Trop. Med. Hyg. 38, 172–180 (1988).

Collins ND, Barrett AD. Live Attenuated Yellow Fever 17D Vaccine: A Legacy Vaccine Still Controlling Outbreaks In Modern Day. Curr Infect Dis Rep. 2017;19(3):14. doi:10.1007/s11908-017-0566-9

Collins, M.H., McGowan, E., Jadi, R., et al. Lack of Durable Cross-Neutralizing Antibodies against Zika Virus from Dengue Virus Infection. Emerging Infectious Diseases 23(5):773-781 (2017). DOI: 10.3201/eid2305.161630

Chao, L.H., Klein, D.E., Schmidt, A.G., Pena, J.M. & Harrison, S.C. Sequential conformational rearrangements in flavivirus membrane fusion *eLife* **3**, e04389 (2014). https://doi.org/10.7554/eLife.04389

Dai L, Wang Q, Song H, Gao GF. Zika Virus Envelope Protein and Antibody Complexes. Subcell Biochem. 2018;88:147-168. doi:10.1007/978-981-10-8456-0_7

Dejnirattisai W, Jumnainsong A, Onsirisakul N, Fitton P, Vasanawathana S, Limpitikul W, Puttikhunt C, Edwards C, Duangchinda T, Supasa S, Chawansuntati K, Malasit P, Mongkolsapaya J, Screaton G. 2010. Cross-reacting antibodies enhance dengue virus infection in humans. Science 328:745–748.

Dejnirattisai, W., Wongwiwat, W., Supasa, S. et al. A new class of highly potent, broadly neutralizing antibodies isolated from viremic patients infected with dengue virus. Nat Immunol 16, 170–177 (2015). https://doi.org/10.1038/ni.3058

Dingens AS, Haddox HK, Overbaugh J, Bloom JD. 2017. Comprehensive mapping of HIV-1 escape from a broadly neutralizing antibody. Cell Host Microbe 21:777–787.e4. https://doi.org/10.1016/j.chom.2017.05.003.

Doud MB, Bloom JD. 2016. Accurate measurement of the effects of all amino acid mutations on influenza hemagglutinin. Viruses 8:155. https://doi.org/10.3390/v8060155.

Dowd KA, DeMaso CR, Pierson TC. Genotypic Differences in Dengue Virus Neutralization Are Explained by a Single Amino Acid Mutation That Modulates Virus Breathing. mBio. 2015;6(6):e01559-15. Published 2015 Nov 3. doi:10.1128/mBio.01559-15

Dussupt, V., Sankhala, R.S., Gromowski, G.D., et al. Potent Zika and dengue cross-neutralizing antibodies induced by Zika vaccination in a dengue-experienced donor. Nature Medicine 26, 228-235 (2020). DOI: 10.1038/s41591-019-0746-2

Goo L, VanBlargan, L.A., Dowd, K.A., Diamond, M.S., Pierson, T.C. A single mutation in the envelope protein modulates flavivirus antigenicity, stability, and pathogenesis. PLoS Pathog. 13(2): e1006178 (2017). https://doi.org/10.1371/journal.ppat.1006178

Guzman, M., Gubler, D., Izquierdo, A. et al. Dengue infection. Nat Rev Dis Primers 2, 16055 (2016). https://doi.org/10.1038/nrdp.2016.55

Halstead SB. Dengue Antibody-Dependent Enhancement: Knowns and Unknowns. Microbiol Spectr. 2014 Dec;2(6). doi: 10.1128/microbiolspec.AID-0022-2014. PMID: 26104444.

Halstead, S. B., Nimmannitya, S. & Cohen, S. N. Observations related to pathogenesis of dengue hemorrhagic fever. IV. Relation of disease severity to antibody response and virus recovered. Yale J. Biol. Med. 42, 311–328 (1970).

Halstead SB. Dengvaxia sensitizes seronegatives to vaccine enhanced disease regardless of age. Vaccine. 2017;35(47):6355-6358. doi:10.1016/j.vaccine.2017.09.089

Huang YJ, Higgs S, Horne KM, Vanlandingham DL. Flavivirus-mosquito interactions.

Viruses. 2014;6(11):4703-4730. Published 2014 Nov 24. doi:10.3390/v6114703

Izmirly AM, Alturki SO, Alturki SO, Connors J, Haddad EK. Challenges in Dengue Vaccines Development: Pre-existing Infections and Cross-Reactivity. Front Immunol. 2020;11:1055. Published 2020 Jun 16. doi:10.3389/fimmu.2020.01055

Katzelnick LC, Gresh L, Halloran ME, et al. Antibody-dependent enhancement of severe dengue disease in humans. Science. 2017;358(6365):929-932. doi:10.1126/science.aan6836

Katzelnick LC, Narvaez C, Arguello S, et al. Zika virus infection enhances future risk of severe dengue disease. Science. 2020;369(6507):1123-1128. doi:10.1126/science.abb6143

Maciejewski S, Ruckwardt TJ, Morabito KM, et al. Distinct neutralizing antibody correlates of protection among related Zika virus vaccines identify a role for antibody quality. Sci Transl Med. 2020;12(547):eaaw9066. doi:10.1126/scitranslmed.aaw9066

Meertens L, Carnec X, Lecoin MP, Ramdasi R, Guivel-Benhassine F, Lew E, Lemke G,

Schwartz O, Amara A. The TIM and TAM families of phosphatidylserine receptors mediate dengue virus entry. Cell Host Microbe. 2012 Oct 18;12(4):544-57. doi: 10.1016/j.chom.2012.08.009. PMID: 23084921; PMCID: PMC3572209.

Metsky, H., Matranga, C., Wohl, S. et al. Zika virus evolution and spread in the Americas. Nature 546, 411–415 (2017). https://doi.org/10.1038/nature22402

Musso D, Bossin H, Mallet HP, Besnard M, Broult J, Baudouin L, Levi JE, Sabino EC, Ghawche F, Lanteri MC, Baud D. Zika virus in French Polynesia 2013-14: anatomy of a completed outbreak. Lancet Infect Dis. 2018 May;18(5):e172-e182. doi: 10.1016/S1473-3099(17)30446-2. Epub 2017 Nov 14. PMID: 29150310.

Navarro-Sanchez E, Altmeyer R, Amara A, Schwartz O, Fieschi F, Virelizier JL, Arenzana-Seisdedos F, Desprès P. Dendritic-cell-specific ICAM3-grabbing non-integrin is essential for the productive infection of human dendritic cells by mosquito-cell-derived dengue viruses. EMBO Rep. 2003 Jul;4(7):723-8. doi: 10.1038/sj.embor.embor866. PMID: 12783086; PMCID: PMC1326316.

Newton ND, Hardy JM, Modhiran N, et al. The structure of an infectious immature flavivirus redefines viral architecture and maturation. Sci Adv. 2021;7(20):eabe4507.

Published 2021 May 14. doi:10.1126/sciadv.abe4507

Pattnaik A, Sahoo BR, Pattnaik AK. Current Status of Zika Virus Vaccines: Successes and Challenges. Vaccines (Basel). 2020;8(2):266. Published 2020 May 31. doi:10.3390/vaccines8020266

Perera-Lecoin M, Meertens L, Carnec X, Amara A. Flavivirus entry receptors: an update. Viruses. 2013;6(1):69-88. Published 2013 Dec 30. doi:10.3390/v6010069

Pierson, T.C., Diamond, M.S. The emergence of Zika virus and its new clinical syndromes. Nature 560, 573–581 (2018). https://doi.org/10.1038/s41586-018-0446-y

Pierson, T.C., Diamond, M.S. The continued threat of emerging flaviviruses. Nat Microbiol 5, 796–812 (2020). https://doi.org/10.1038/s41564-020-0714-0

Polack FP, Thomas SJ, Kitchin N, et al. Safety and Efficacy of the BNT162b2 mRNA Covid-19 Vaccine. N Engl J Med. 2020;383(27):2603-2615. doi:10.1056/NEJMoa2034577

Rawal G, Yadav S, Kumar R. Zika virus: An overview. J Family Med Prim Care. 2016;5(3):523-527. doi:10.4103/2249-4863.197256

Sabchareon, A. et al. Protective efficacy of the recombinant, live-attenuated, CYD tetravalent dengue vaccine in Thai schoolchildren: a randomised, controlled phase 2b trial. Lancet 380, 1559–1567 (2012).

Schwarz MC, Sourisseau M, Espino MM, et al. Rescue of the 1947 Zika Virus Prototype Strain with a Cytomegalovirus Promoter-Driven cDNA Clone. mSphere. 2016;1(5):e00246-16. Published 2016 Sep 28. doi:10.1128/mSphere.00246-16

Sesterhenn F, Bonet J, Correia BE. Structure-based immunogen design-leading the way to the new age of precision vaccines. Curr Opin Struct Biol. 2018;51:163-169. doi:10.1016/j.sbi.2018.06.002

Simmons CP, Chau TN, Thuy TT, Tuan NM, Hoang DM, Thien NT, Lien le B, Quy NT, Hieu NT, Hien TT, McElnea C, Young P, Whitehead S, Hung NT, Farrar J. 2007. Maternal antibody and viral factors in the pathogenesis of dengue virus in infants. J Infect Dis 196:416–424.

Sirohi D, Kuhn RJ. Zika Virus Structure, Maturation, and Receptors. J Infect Dis. 2017 Dec 16;216(suppl_10):S935-S944. doi: 10.1093/infdis/jix515. PMID: 29267925; PMCID: PMC5853281.

Slon-Campos, J.L., Dejnirattisai, W., Jagger, B.W. et al. A protective Zika virus E-dimer-based subunit vaccine engineered to abrogate antibody-dependent enhancement of dengue infection. Nat Immunol 20, 1291–1298 (2019). https://doi.org/10.1038/s41590-019-0477-z

Sourisseau M, Lawrence DJP, Schwarz MC, Storrs CH, Veit EC, Bloom JD, Evans MJ. 2019. Deep mutational scanning comprehensively maps how Zika envelopE protein mutations affect viral growth and antibody escape. JVI Vol 93, No 23. https://doi.org/10.1128/JVI.01291-19

Swanstrom, J.A., Plante, J.A., Young, E.F., et al. Dengue virus Envelope Dimer Epitope (EDE) monoclonal antibodies isolated from dengue patients are protective against Zika virus. MBio 7(4). DOI: 10.1128/mBio.01123-16

Vannice KS, Cassetti MC, Eisinger RW, et al. Demonstrating vaccine effectiveness during a waning epidemic: A WHO/NIH meeting report on approaches to development

and licensure of Zika vaccine candidates. Vaccine. 2019;37(6):863-868. doi:10.1016/j.vaccine.2018.12.040

Welsch S, Miller S, Romero-Brey I, Merz A, Bleck CK, Walther P, Fuller SD, Antony C, Krijnse-Locker J, Bartenschlager R. Composition and three-dimensional architecture of the dengue virus replication and assembly sites. Cell Host Microbe. 2009 Apr 23;5(4):365-75. doi: 10.1016/j.chom.2009.03.007. PMID: 19380115; PMCID: PMC7103389.

Zhang Q, Sun K, Chinazzi M, et al. Spread of Zika virus in the Americas. Proc Natl Acad Sci U S A. 2017;114(22):E4334-E4343. doi:10.1073/pnas.1620161114